Atomic Force Microscopy

Thesis · May 2017

DOI: 10.13140/RG.2.2.17356.10887

1 author:

Bob Kyeyune
Osnabrück University
4 PUBLICATIONS **6** CITATIONS

SEE PROFILE

Atomic Force Microscopy

Bob KYEYUNE (bob@aims.ac.tz)
AIMS161700617

African Institute for Mathematical Sciences (AIMS)

Supervised by: Professor Erkki Lähderanta
Lappeenranta University Of Technology, Finland

31st May 2017

Submitted in partial fulfillment of a structured masters degree at AIMS Tanzania

Abstract

Characterizing a material with its properties such as electrical properties, mechanical properties and chemical properties at a nano scale has become key to understand the nature of a material. Atomic force microscopy (AFM) plays a big role to experimentally measure these properties. In this report, an overview is given, the working principle of the atomic force microscopy with its working modes, which is the static and dynamic modes. The equation of motion of the cantilever is studied and the amplitude of oscillation, the frequency shift and phase are obtained. Leonard Jones potential is discussed. It characterizes the repulsive and attractive forces during the tip sample interaction. Pauli exclusion principle contributes to the repulsive forces between the tip sample interactions. Some attractive forces like Van dar Waals, electrostatic forces, capillary forces and magnetic forces are discussed. Employing Kelvin probe force microscopy, the work function of the material can be measured both in the amplitude modulation (AM) and the frequency modulation (FM). Next to Kelvin probe microscopy, we also discuss the Bruker multimode 8 AFM (BMM8) and its PeakForce tapping mode (PFT) and the automatic parametrization using PeakForce ScanAsyst, with its different imaging modes like PeakForce QNM where quantitative nanomechanical imaging is allowed.The Derjanguin-Muller-Toporov (DMT) model for extracting the elastic modulus is discussed, PeakForce TUNA which allows for the characterization of conductivity of a material and PeakForce KPFM which combines KPFM with PeakForce technique.

Keywords: Atomic force microscopy, topography, resonance frequency, calibration, mechanical properties, PeakForce, interaction forces

Declaration

I, the undersigned, hereby declare that the work contained in this research project is my original work, and that any work done by others or by myself previously has been acknowledged and referenced accordingly.

Bob Kyeyune, 31st May 2017

Contents

List of Figures

1. Introduction

Atomic force microscopy (AFM) is an advanced technique of studying properties of materials at an atomic scale. The technique has played a big role in fields of science like material science, molecular biology and solid-state physics. It arose from the scanning tunnelling microscopy (STM). STM was invented in 1982 by Binning and co-workers (Binnig et al., 1982) to investigate surfaces of conductive materials. STM was limited to only conductive materials like metals and semiconductors. In order to study non-conductive materials, AFM was invented in 1986 by G.Binning, C.F.Quate and Ch.Gerber (Binnig et al., 1986).

The group focused on studying the force between the tip and the sample in the contact mode rather than the tunnelling currents. Binning and his group incorporated a spring-like cantilever to hold the tip. The cantilever was made out of a thin gold (Au) foil with a diamond tip. The cantilever adjusts the tip to the sample surface. The experimental set up of the approach depicted in the review letter (Binnig et al., 1982) is shown in Figure 1.1. The cantilever is between the sample and the tip, it is fixed to a modulating piezo E it can be seen in Figure 1.1.

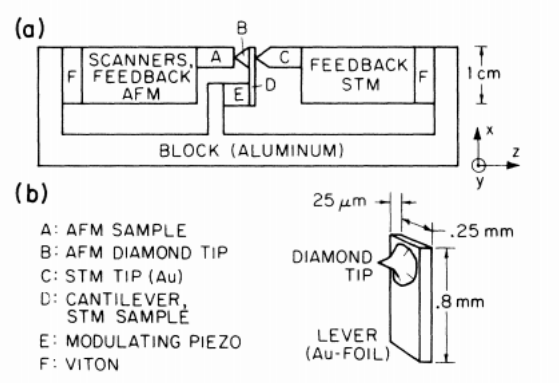

Figure 1.1: An experimental set up of the STM with an incorporated gold cantilever is shown. The dimensions of the cantilever is depicted in the lower right corner.

The study of interaction force was quite successful in investigating properties of materials. This has led to new invention of scanning techniques such as the Magnetic force microscopy (MFM). MFM which images the magnetic properties of magnetic samples was invented in 1987 (Martin and Wickramasinghe, 1987). The experiment was based on imaging magnetic fields with $100\mathring{A}$ resolution. Kelvin probe force microscopy (KPFM) is another example. The technique was first introduced in 1991 (Nonnenmacher et al., 1991). It is known for mapping the surface electrical properties such as the work function of a material, for-example semiconductors, on a nano-meter scale. The technique combines the abilities of AFM and the Kelvin probe technique. The Kelvin probe was an invention in 1898 by Lord Kelvin (Sadewasser and Glatzel, 2012) where he studied a set of vibrating parallel plates with different Fermi energies. A current was measured between the plates due to changes in capacitance between the plates with a fixed voltage between the plates.

From the first AFM invention, there have been very many improvements. These further developments led to the dynamic mode. In 1993, the tapping mode was developed (Zhong et al., 1993) where, the cantilever was oscillated near its resonance frequency. In this mode the force of interaction is minimised, which reduces sample damage from lateral forces. The mode allows for high resolution mapping.

In 2010, Bruker introduced PeakForce tapping mode. The technique is similar to AFM tapping mode. The mode was introduced to improve the resolution of the AFM using forces on a pico-Newton scale (Pittenger et al., 2010). The technique allows to extract different properties in each tapping cycle from a single sample. The mode allows for multiple imaging modes like PeakForce QNM, PeakForce TUNA, and PeakForce KPFM. Alongside these modes, the PeakForce ScanAsyst provides an automatic adjustment of the imaging parameters. From the recent efforts to study the intrinsic properties of amyloid fibrils (Adamcik et al., 2012), PeakForce QNM demonstrated high efficiency in characterizing the elastic modulus of amyloid fibrils independent of the polymorphic state and the cross-sectional structure details.

Within the proposed experimental work connected to this work, semiconductor nanowires from III-V semiconductor materials for solar cells, nanogenerators of electric current, photodetectors. More specifically semiconductor nanowires for thin film solar cells are most likely to be considered. Further experimental studies may help to increase efficiency of solar cells and to have an inexpensive energy source accessible to many. This has motivated my choice of this research area.

To summarize, studying materials at a nano-scale provides a greater surface area per mass of a material than at a micro or larger scale. The large surface area enables a large portion of the material to be in contact with the probe. Therefore, enough information about the properties of a sample can be extracted. It is this information extracted at nano scale that has caught researchers' attention. AFM was initially used to image the topography of a material, but due to the various developments in AFM a variety of properties like elastic modulus, surface potential, electric current, adhesion, deformation, friction, capacitance and magnetic properties can be studied.

In this work, we give an overview over the basics of AFM. The guiding objectives of this work are;

- To describe the basic working principle of AFM.
- To give an overview over the working modes of AFM.
- To describe the mechanism of Kelvin probe force microscopy.
- To describe Bruker's PeakForce tapping mode and its multi-imaging modes.

In chapter (2), we discuss the basic working principle of AFM and its working modes, which are, static and dynamic modes. Furthermore we study the motion of the cantilever with the assumption that it is a spring-like cantilever and the Lennard Jones interaction potential. In chapter (3), the forces of interactions such as Van der Waals interaction forces, electrostatic forces, capillary forces and magnetic forces between the tip and the sample are discussed. In chapter (4), the AFM KPFM is discussed. For this purpose, the electrostatic force and electrostatic force gradient are considered. It describes how the contact potential difference (CPD) is measured in the tapping mode. In this chapter we also look at the amplitude and frequency modulation modes. In chapter (5), we introduce the Bruker multimode 8 microscope, its PeakForce tapping and PeakForce ScanAsyst where automatic parametrization is allowed. Multi imaging modes like the PeakForce QNM where quantitative mechanical measurements are conducted, PeakForce TUNA where conductivity of a material at high resolution is considered, and PeakForce KPFM where surface potential at high resolution can be measured are discussed.

2. Atomic Force Microscopy

2.1 Basic Working Principles

Atomic force microscopy (AFM) is a technique that is used to map the topography and to study the properties of material on a nanoscale. AFM uses a probing tip at one end of a spring-like cantilever to interact with the material (sample). The interaction between the sample and the tip gives rise to either attractive or repulsive forces. These forces give information about the topography of the sample. If the tip and the sample are close to each other, the attractive force deflects the cantilever towards the sample, and when the tip is brought into contact with the sample, the repulsive force deflects the cantilever away from the sample. This phenomena can be explained by the Pauli exclusion principle.

The cantilever system acts as the force sensor. The cantilevers comes in different shapes, the choice depends on the kind of measurements to be conducted. In order to have a small sensitivity to the force, a spring constant k is chosen in the range of $0.01 - 100\frac{N}{m}$ (Meyer, 1992). For cases of vibrations of the cantilever, the cantilever is vibrated at the resonant frequency. Since the resonance frequency is dependent on the force constant and the mass of the cantilever as in Equation (2.3.1), this means the mass of the cantilever has also to be minimised. This is done by reducing its dimensions.

A laser beam detects these deflections. This happens when the incident laser beam is reflected off the surface of the cantilever, any deflection will cause changes of the direction of the reflected beam.

A high resolution deflection detector (position sensitive detector) is used to register these change. The changes can either be large or small. The detector is sensitive enough that to amplify even the very small deflections.

The feedback loop maintains a predefined setpoint that is determined by the instrument. In this case, the feedback controls the deflection of the cantilever.

The piezoelectric XYZ-scanner is responsible for the movements between the tip and sample in the x,y,z-directions. The piezoelectric scanner gives us the access to do imaging in three dimension. The schematic diagram of the working principle of the AFM is shown in the Figure 2.1.

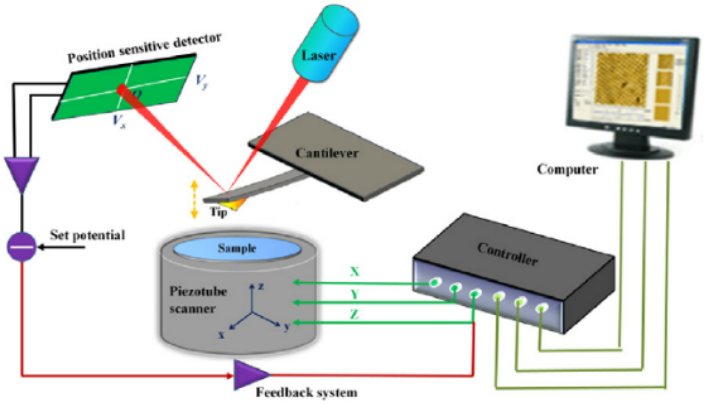

Figure 2.1: A schematic diagram for the working principle of AFM, where the probing tip-sample interaction gives rise to the cantilever deflection. The diagram is taken from (Quenet)

.

The AFM operates in two general modes, the static mode also known as the contact mode and the dynamic mode (the non-contact mode and the tapping mode). In each of the modes, there is a dominant interaction forces. The repulsive forces are seen in the contact mode, the attractive forces force are observed in the non-contact mode. In the tapping mode at high frequencies we can see both the repulsive and the attractive mode.

2.2 Cantilever Calibrations

AFM makes force measurements which majorly depends on the cantilever and tip properties like the spring constant, deflection sensitivity, quality factor, resonance frequency and the tip size and shape. A part from the imaging done by the microscope, AFM has the ability to give quantitative information about the interaction between the tip and the sample. The accuracy of the quantitative measurements made are dependent on the knowledge of spring constant k and the corresponding resonance frequency, the deflection sensitivity and the tip size and shape. Therefore, this calls for calibration of these factors. Here, we discuss the calibration of the spring constant and the resonance frequency, deflection sensitivity and shape and size of the tip.

Spring constant calibrations

Calibrations of the spring constant can be done in different ways like the geometrical method and thermal noise method. We discuss the thermal noise here. For a cantilever undergoing harmonic oscillations in equilibrium with the surroundings, the oscillations will reduce due to thermal noise. We can write the Hamiltonian of such a system as,

$$H = \frac{p^2}{2m} + \frac{1}{2}m\omega_0^2 z^2, \tag{2.2.1}$$

where p is the momentum of the system, m the oscillating mass, z the displacement of the oscillation and ω_0 is the resonance frequency.

The method uses the equipartition theorem to determine the spring constant. The theorem states that in thermal equilibrium the average energy value of each quadratic term in the Hamiltonian is equal to $\frac{1}{2}k_BT$ (García, 2011), i.e,

$$\langle\frac{1}{2}m\omega_0^2 z^2\rangle = \frac{1}{2}k_BT. \tag{2.2.2}$$

But the resonance frequency $\omega_0 = \sqrt{\frac{k}{m}}$. Therefore Equation (2.2.2) becomes,

$$\frac{1}{2}k\langle z^2\rangle = \frac{1}{2}k_BT. \tag{2.2.3}$$

If the average mean square of deflection $\langle z^2\rangle$ is known, then the spring constant can be given as

$$k = \frac{k_BT}{\langle z^2\rangle}, \tag{2.2.4}$$

where T is the temperature of the cantilever and k_B is the Boltzmann constant.

Deflection sensitivity calibration

The calibration of the deflection sensitivity is conducted by converting the photodiode signals measured in volts to nanometres García (2011). This is achieved by obtaining a calibration factor in units of

Vnm^{-1}. A force curve of photodiode signals (volts) against the displacement of the cantilever (nm). The slope of the curve is obtained and it is the calibration factor

$$\sigma = \frac{\triangle V}{\triangle z}, \tag{2.2.5}$$

where z is cantilever displacement in the vertical direction, V is the voltage measured from the photodiode.

Calibration of the shape and size of the tip

Tips come commonly in three different shapes such as cone, pyramid and sphere. To calibrate the size and shape of a tip, one can use plastic indentation. In plastic indentation you take a soft material (sample), push hard the tip into it. Now with a low force, image the hole that is created in the sample. Usually the cantilever has a slight angle with respect to the sample. This means the hole created in the sample may not be a perfect hole. In this case we require to have horizontal cantilever with the tip normal to the sample. This will provide a relatively perfect hole which when imaged the shape and size of the tip can be obtained.

2.3 Working Modes

As seen already, AFM works in the static mode also known as the contact mode and the dynamic mode where we have both the non-contact and tapping modes. We differentiate between the two dynamic modes in this section though some authors treat the non-contact and tapping modes to be the same.

2.3.1 Contact Mode. In the contact mode, the AFM is at its simplest working mode. Here the cantilever is adjusted until the sample and the probing tip are in contact. The deflection of the cantilever

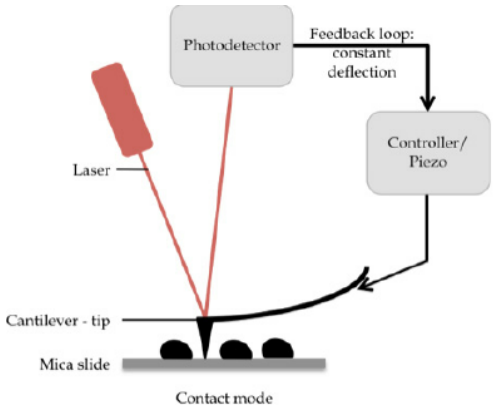

Figure 2.2: The working principle of AFM in contact mode, where the tip contacts the sample surface with a small cantilever deflection and the feedback loop keeps the deflection constant. Therefore we have a constant force. Figure is taken from (Quenet)

,

is measured. If we denote the deflection by δz then the corresponding force is proportional to the deflection

$$F = -k\delta z.$$

This is obtained from Hook's law since we consider the cantilever as a spring, where k is the force constant. The tip-sample interacting forces are in the repulsive regime which can be seen in figure 3.1 in subsection 3.1.

In this mode the feedback loop keeps the deflection of the cantilever constantly at the set-point.The set-point is a value set by the operator of the microscope. Its one of the parameters among others that the operator has to monitor to optimize the imaging. This unchanged deflection can also be referred to as the equiforce mode (Meyer, 1992). Figure 2.2 illustrates the probing tip and the sample in contact and the feedback loop maintaining a constant deflection.

The contact mode has the disadvantage that, both the sample and the tip may experience damages due to lateral forces.

2.3.2 Dynamic mode. In general, in the dynamic mode the vibration amplitude of the cantilever is measured to estimate the deflection of the cantilever. AFM working in this mode is called the amplitude modulation AFM (AM-AFM). Within the frequency modulation technique (FM-AFM), the shift of the resonance frequency is measured (Seo and Jhe, 2007). The attractive and repulsive forces give rise to changes in the amplitude and frequency. For the amplitude modulation mode, the change in amplitude is used as the feedback signal that gives information about the topography of the sample. This change in amplitude is dependent on the tip-sample interaction force and this change is monitored by a feedback loop to keep the tip-sample distance constant.

In the frequency Modulation (FM) mode, the change in frequency gives the information about the tip-sample interactions and the feedback loop monitors the frequency change.These frequency changes are dependent on the force gradient $\frac{dF_{ts}}{dz}$ where F_{ts}, is the tip-sample force. The resonance of the cantilever is characterized by three different parameters: amplitude, frequency and the phase shift. We can try to analytically understand these parameters from the equation of motion of the cantilever.

Non-Contact Mode

In this mode the tip is brought close to the sample in a constant distance. The tip is oscillated at or near its resonance frequency,

$$\omega_0 = \sqrt{\frac{k}{m}}, \tag{2.3.1}$$

where k is the spring constants of the cantilever, m is the mass of the spring-like cantilever. These oscillations are mechanically excited by the system on which the cantilever is mounted. The cantilever must be stiffer than in the contact mode, this allows the cantilever to have a small bending and a high force sensitivity. The interacting forces are in the attractive regime. These forces are very weak that they support imaging of soft samples unlike in the contact mode where soft samples are likely to be damaged due to the close contact.

Due to the varying shape of the sample, during interactions between the tip and sample surface, the cantilever oscillates with different amplitudes. A feedback loop is used to cater for theses anomalies to have a constant amplitude.

Tapping Mode

In the tapping mode, the cantilever oscillates at the resonance frequency but at intermittent contact unlike in the non-contact mode where there is no contact at all. The vibration is set at the resonant frequency with a constant fixed amplitude. If this amplitude is kept small, that is approximately 1nm, the tip-sample interacting force will be in the attractive regime. If the amplitude is kept at a large value say at about 100nm, then the tip-sample interacting force can reach the repulsive regime.

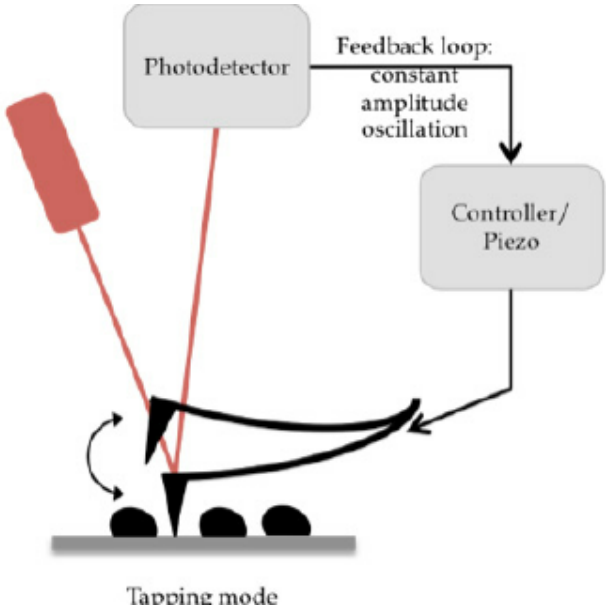

Figure 2.3: The Principle working mechanism of atomic force microscopy in tapping mode, with an oscillating cantilever, the photodetector output signal is analyzed to obtain the amplitude and phase of the cantilever oscillation. The feedback loop keeps the oscillation amplitude constant. Figure taken from (Quenet)

2.4 Motion of The Cantilever

The equation of motion can be studied in two ways. One can consider the cantilever as a beam with a massless probing tip or considering the cantilever to be of spring-type. In this work we focus on the second case where the cantilever is assumed to be a 1-dimensional point mass spring of mass m and spring constant k with deflection in the z-direction. Figure 2.4 is illustrates a cantilever with some forces acting on it.

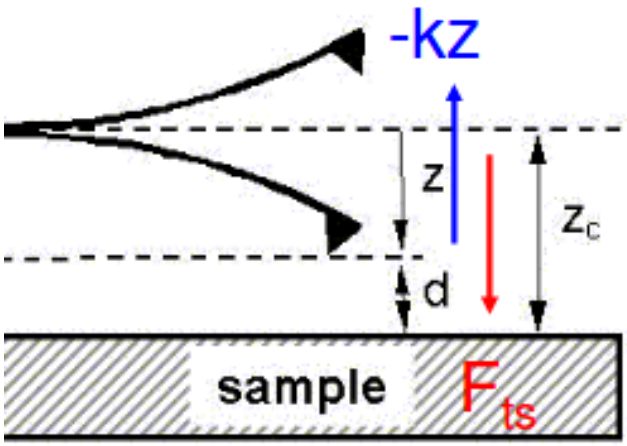

Figure 2.4: A figure showing the deflection of a cantilever in the z-direction. Figure is taken from (Perez)

Figure 2.4 shows the tip-sample interacting force F_{ts}. Due to the spring-type nature, the force propor-

tional to the deflection z, $F = -kz$ acts on the cantilever. Though not indicated in the figure we have a force driving the oscillation. It is given by $F_0 \cos \omega t$, where F_0 is the amplitude of oscillation and ω is the frequency of the oscillation. We also have the hydrodynamic force $F_h = \frac{m\omega_0}{Q}\dot{z}$, which is the resistance that may arise due interactions with a fluid, where Q is the quality factor. It is defined as the measure of energy loss of the oscillation and it is given by Melitz et al. (2011)

$$Q = \frac{\omega_0}{\triangle\omega}, \tag{2.4.1}$$

where ω_0 is the resonant frequency of the cantilever and $\triangle\omega$ is the change in frequency. Now with these forces, we can write the equation of motion from the Newton's second law of motion as

$$m\ddot{z} + b\dot{z} + kz = F_{ts} + F_0 \cos \omega t, \tag{2.4.2}$$

where $b = \frac{m\omega_0}{Q}$.

We define the resonance frequency as seen in Equation (2.3.1). Solving this equation By assuming absence of tip-surface forces, i.e, $F_{ts} = 0$ and from this Equation (2.4.2) becomes,

$$\ddot{z} + \gamma\dot{z} + w_0^2 z = \frac{F_0}{m} \cos \omega t, \tag{2.4.3}$$

where $\gamma = \frac{b}{m}$.

We are interested in obtaining the three parameters, amplitude, frequency and the phase shift, but we know that amplitude depends on the driving force. The solution to the differential Equation (2.4.3) consists of a particular solution and the complimentary solution to the steady and transient terms of the differential equation respectively,

$$z(w, t) = z_p(\omega, t) + z_c(\omega, t). \tag{2.4.4}$$

For the steady term, if we write $\cos \omega t = Re\left[e^{iwt}\right]$, then we choose an ansatz $Z = Ae^{iwt}$. From which we can obtain our desired amplitude A. If we substitute Z into Equation (2.4.3) we obtain

$$-A\omega^2 e^{iwt} + \gamma A i\omega e^{iwt} + \omega_0^2 A e^{iwt} - \frac{F_0}{m} e^{iwt} = 0. \tag{2.4.5}$$

If we put terms together we obtain

$$e^{iwt}\left(A(-\omega^2 + \gamma A i\omega + \omega_0^2) - \frac{F_0}{m}\right) = 0. \tag{2.4.6}$$

Now, if we make A the subject we obtain

$$A = \frac{\frac{F_0}{m}}{\left(w_0^2 - w^2\right) + iw\gamma}. \tag{2.4.7}$$

With $\gamma = \frac{b}{m} = \frac{w_0}{Q}$, we can rewrite (2.4.7) as,

$$A = \frac{\frac{F_0}{m}}{\left(w_0^2 - w^2\right) + iw\frac{w_0}{Q}}. \tag{2.4.8}$$

Now, the magnitude of the amplitude $|A|$ is given as

$$|A(w)| = \frac{\frac{F_0}{m}}{\sqrt{\left(w_0^2 - w^2\right)^2 + w^2 \frac{w_0^2}{Q^2}}}. \tag{2.4.9}$$

This amplitude depends on the driving frequency ω.

The corresponding phase shift ϕ is given by

$$\phi = \arctan\left(\frac{\frac{ww_0}{Q}}{w_0^2 - w^2}\right). \tag{2.4.10}$$

ϕ is the angle by which the cantilever is displaced by the driving force.

If the angular frequency is the resonance frequency, i.e. $\omega = \omega_0$, then Equation (2.4.9) becomes

$$|A(\omega = \omega_0)| = \frac{QF_0}{k}. \tag{2.4.11}$$

Therefore, at the resonance frequency the amplitude of the cantilever is given by Equation (2.4.11) and is dependent on the force constant, the quality factor Q and the amplitude of the driving force.

We can write the solution to the steady part as,

$$z_p = Re\left[|A|e^{iwt}e^{-i\phi}\right]$$

$$= \frac{\frac{F_0}{m}}{\sqrt{\left(w_0^2 - w^2\right)^2 + w^2 \frac{w_0^2}{Q^2}}} \cos(wt - \phi). \tag{2.4.12}$$

The solution to the homogeneous part of Equation (2.4.3) is given by

$$z_c(\omega, t) = Be^{-\alpha t}\cos(\omega_d t + \beta), \tag{2.4.13}$$

where $\alpha = \frac{\omega_0}{2Q}$ and the resonance angular frequency is related to the free resonance as

$$\omega_d = \omega_0\left(1 - \frac{1}{4Q^2}\right)^{\frac{1}{2}}. \tag{2.4.14}$$

If we assume $F_{ts} > 0$, the new effective spring constant k_e is given by

$$k_e = k - \frac{dF_{ts}}{dz}. \tag{2.4.15}$$

And from Equation (2.4.15) we can deduce the modified resonance frequency as,

$$\tilde{\omega} = \sqrt{\frac{k_e}{m}} = \sqrt{\frac{k - \frac{dF_{ts}}{dz}}{m}} = \omega_0\sqrt{1 - \frac{\frac{dF_{ts}}{dz}}{k}}. \tag{2.4.16}$$

What Equation (2.4.16) conveys is that the resonance frequency of a perturbed oscillating cantilever by a weak force F_{ts} depends on the force gradient $\frac{dF_{ts}}{dz}$. During the interactions between the vibrating

cantilever and the sample, there is a shift in the resonance frequency caused by the force gradient. This shift can be determined to be

$$\triangle\omega = \tilde{\omega} - \omega_0 = \omega_0 \left\{ \left(\sqrt{1 - \frac{F'_{ts}}{k}} \right) - 1 \right\}. \tag{2.4.17}$$

If we use Taylor expansion of equation (2.4.17) we obtain,

$$\triangle\omega = -\omega_0 \frac{F'_{ts}}{2k}. \tag{2.4.18}$$

Depending on the shift in the angular frequency, we can determine whether the force of interaction is either repulsive or attractive.

For attractive potential, the force gradient is positive (i.e. $F'_{ts} > 0$) which implies that the resonance frequency shift is negative (i.e. $\triangle\omega < 0$) and for the repulsive potential, the resonance frequency shift is positive.

An illustration of amplitude depending on the frequency for different F_{ts} is shown in the Figure (2.5),

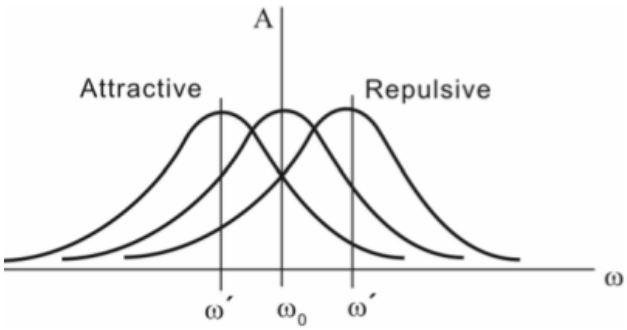

Figure 2.5: An illustration of amplitude depending on the frequency for different F_{ts}. Image is taken from (Seo and Jhe, 2007), we reffer to $\tilde{\omega}$ as ω'

.

3. Tip-sample Interaction Forces

3.1 Potential Versus Distance Curves

When the probing tip approaches the sample surface, there exists interaction forces between the sample and the tip to which many possible forces contribute. The forces are classified into repulsive and attractive forces.

Employing the Lennard-Jones interaction potential, the total potential comprising the attractive and the repulsive part is given as (Sadewasser and Glatzel, 2012)

$$U_{LJ} = 4\epsilon \left(\left(\frac{\sigma}{r} \right)^{12} - \left(\frac{\sigma}{r} \right)^{6} \right), \tag{3.1.1}$$

where ϵ is the the depth of the potential well.

For cases where we have a short-range separation between the tip and the sample, the resulting force is the repulsive force and is described by the interacting potential(Sadewasser and Glatzel, 2012)

$$U_{repulsive} = 4\epsilon \left(\frac{\sigma}{r} \right)^{12}. \tag{3.1.2}$$

Now if the tip-sample separations are larger, then the interaction potential is attractive, given as

$$U_{attractive} = -4\epsilon \left(\frac{\sigma}{r} \right)^{6}. \tag{3.1.3}$$

The figure below shows a plot for the potential as a function of the tip-sample separation with choice of $\epsilon = 2.0$ and $\sigma = 2.7$.

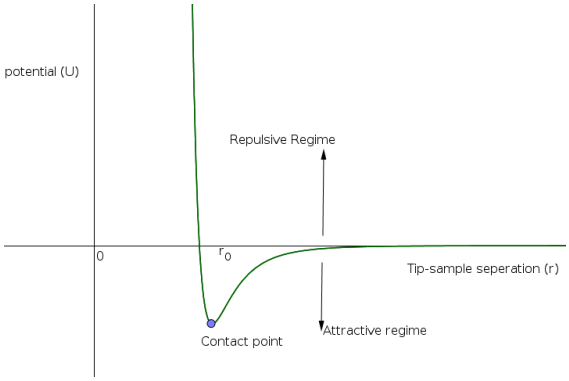

Figure 3.1: A plot of the Lennard-Jones potential as a function of the tip-sample separation that shows the regimes of acting forces between the tip and the sample.

As discussed earlier if the AFM is operating in the static mode (contact mode), then the associated interaction forces which we call short-range forces are found in the repulsive regime. For the dynamic mode we can find the forces of interaction in the attractive and repulsive regime for low and high amplitude vibrations, respectively.

The existence of the repulsive forces at very small inter-atomic separations can be best explained by the Pauli exclusion principle.

3.2 Repulsive Forces With The Pauli Exclusion Principle

When the tip-sample separations are so small that the electron orbitals start to overlap, we say that atoms are interacting with an inter-atomic spacing. According to the Pauli exclusion principle, two electrons can not exist in the same quantum state, which explains the existence of a repulsive force. We can model these electrons as indistinguishable identical particles. For each particle, we have a states with its respective quantum numbers (principal quantum number (n), angular quantum number (l), magnetic quantum number (m) and the spin (s)) denoted by k_i with $i = 1, 2, \cdots, N$. We can write the N-particle states as a linear combination of products of the single particle states. We define $|\psi_N\rangle$ as the product of the of the single particle states denoted by

$$|\psi_N\rangle = |\psi_{k_1}, \psi_{k_2}, \cdots, \psi_{k_N}\rangle = |\psi_{k_1}\rangle|\psi_{k_2}\rangle \cdots |\psi_{k_N}\rangle. \tag{3.2.1}$$

The N-particle states for these identical particles are either symmetric or anti-symmetric for the bosons and fermions, respectively.

More generally, this means that a basis state of N identical particles must satisfy (Reichl, 2016)

$$|\psi_N^{\pm}\rangle = \frac{1}{\sqrt{N!}} \sum_{\mathcal{P}} (\pm 1)^p \mathcal{P} \left(|\psi_{k_1}\rangle|\psi_{k_2}\rangle \cdots |\psi_{k_N}\rangle\right), \tag{3.2.2}$$

where $|\psi_N^{\pm}\rangle$ is the state for either the symmetric or the anti-symmetric particles. $\mathcal{P}$ is any permutation of the N particles, summing over $N!$ possible permutation and p are the number of pairwise exchanges making up $\mathcal{P}$. The $|\psi_N^{+}\rangle$ is representing the symmetric states and $|\psi_N^{-}\rangle$ the anti-symmetric states. Now consider two indistinguishable particles in the states $|\psi_{k_1}\rangle$ and $|\psi_{k_2}\rangle$. Here we will only consider the anti-symmetric state because we are only interested in the electrons which are fermions. In this case the two-particle normalised state is expressed as

$$|\psi_2^{-}\rangle = \frac{1}{\sqrt{2}} \left(|\psi_{k_1}\rangle|\psi_{k_2}\rangle - |\psi_{k_2}\rangle||\psi_{k_1}\rangle\right). \tag{3.2.3}$$

If $|\psi_{k_2}\rangle = |\psi_{k_1}\rangle$,

$$|\psi_2^{-}\rangle = 0.$$

This is the Pauli exclusion principle, which posits that two fermions cannot exist in the same quantum state. This result is shows that we cannot have two electrons with the same quantum numbers in the same quantum state. In this case electrons will repel one from the other thus creating a degenerate repulsive force.

Other Interaction Forces

In AFM, when a tip approaches the sample, interaction forces arise. We use the forces of interactions between the probing tip and the sample to understand the physical properties of the sample. We have already mentioned that these forces can be categorized into the repulsive forces and the attractive forces. For the attractive forces we consider the Van der waal interactions, electrostatic forces, capillary forces and magnetic forces.

3.3 Van der Waals Interactions

These forces play an important role considering the interaction forces in AFM experiments (Meyer, 1992). They can be divided into three different types of interactions (Israelachvili, 2011) which are Keeson Dipole force, Debye dipole force and the London dispersion force. The Keeson dipole force originate from dipole-dipole interactions, the Debye dipole forces originate from the interaction of a dipole with an induced dipole and they increase with the polarizability, which can be seen by $P = \alpha E$ (Israelachvili, 2011), where P is the induced dipole moment, α is the polarizability and E the electric field. The London dispersion forces result from the interaction of two temporary dipoles, they increase with the area of contact between the molecules and the polarizability. The potential energy U of each of these interactions scales with $\frac{1}{r^6}$ where r is the separation between the atoms. Therefore, the total contribution of the Van der waals interaction can be described by a potential which scales with $\frac{1}{r^6}$. From the potential-force relation

$$\mathbf{F} = -\nabla U, \tag{3.3.1}$$

we find that the corresponding force **F** through the relation (3.3.1) scales with $\frac{1}{r^7}$. **F** is the force of a single dipole. Now, to find the total force F of interaction between the tip and the sample we consider a continuous medium where we integrate over the tip and the sample, as in Equation (3.3.2)

$$F = \int_{v_t} \int_{v_s} \rho_t dV_t \rho_s \mathbf{F} dV_s, \tag{3.3.2}$$

where v_t and v_s are the volumes for the tip and the sample, respectively, and the corresponding densities as ρ_t and ρ_s. The nature of this force is attractive and depends on the geometry of the tip.

3.4 Electrostatic Forces

In atomic force microscopy, electrostatic forces arise from interactions of a charged tip and sample. If we model our tip and sample as a parallel plate capacitor with charge Q of equal magnitude for each plate separated by a distance z, with cross sectional area A and ϵ_0 as the permittivity of vacuum, we can then write the capacitance C as

$$C = \frac{Q}{\triangle v} = \frac{A\epsilon_0}{z}, \tag{3.4.1}$$

where $\triangle v$ is the potential difference between the samples and the tip. Then the force between the sample and the tip is given as $F = QE$, where $E = \frac{Q}{\epsilon_0 A}$, therefore

$$F = Q\frac{1}{2}\frac{Q}{\epsilon_0 A} = \frac{1}{2}\frac{\epsilon_0 A}{z^2}\triangle v^2. \tag{3.4.2}$$

From Equation (3.4.1) we obtain that $\frac{\partial C}{\partial z} = -\frac{\epsilon_0 A}{z^2}$. Therefore the force between the tip and the sample can be expressed as

$$F = \frac{1}{2}\frac{\epsilon_0 A}{z^2}\triangle v^2 = -\frac{1}{2}\frac{\partial C}{\partial z}\triangle v^2. \tag{3.4.3}$$

Note that $\frac{\partial C}{\partial z}$ in general depends on the geometry of the tip and the sample. We only need to know the ratio $\frac{\partial C}{\partial z}$ and we make use of Equation (3.4.3) to obtain the electrostatic force between the tip and the sample. These electrostatic forces are attractive forces and they are detectable at a separation where $z \geq 10$nm (Meyer, 1992).

3.5 Capillary Forces

In atomic force microscopy, we observe capillary forces when a hydrophilic surface absorbs water molecules in ambient conditions. When the probing tip is brought in close contact with the water surface, a meniscus is formed, see Figure (3.2), which creates a strong attraction force between the tip and the water molecules.

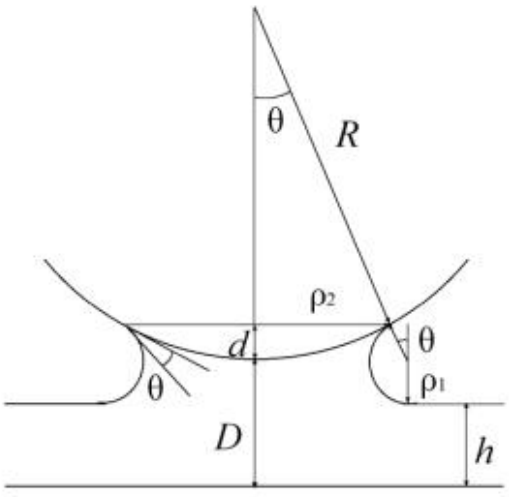

Figure 3.2: The meniscus between a spherical probe and a liquid film.

Young's non-linear partial differential equation describes the interaction pressure between the probe and the liquid sample (Eijkel and Van Den Berg, 2005),

$$\triangle p = \sigma \left(\frac{1}{\rho_1} + \frac{1}{\rho_2} \right) = \frac{\sigma}{r_k}, \tag{3.5.1}$$

where σ is the surface tension and r_k is called the kelvin radius and is given by

$$r_k = \frac{1}{\left(\frac{1}{\rho_1} + \frac{1}{\rho_2} \right)}.$$

ρ_1 and ρ_2 are the radii of curvatures depicted in Figure 3.2. The resulting attractive force F is given by

$$F = 2\pi R d \triangle p = 2\pi R d \frac{\sigma}{r_k}, \tag{3.5.2}$$

where $2\pi Rd$ is the contact area between the liquid sample and the probe, d the depth of the probe into the liquid and R the radius of the probing tip.

If we assume that $\rho_1 << \rho_2$, we obtain that $r_k \approx \rho_1$. Furthermore, using trigonometry we can infer $\rho_1 \cos\theta + \rho_1 = D + d - h$ from the sketch. With the assumption that the height of the liquid film is negligible, i.e., $h = 0$ and $D = 0$, the resulting force is given as, $F = 4\pi R\sigma \cos\theta$. For small angles of θ we can approximate $\cos\theta \simeq 1$. Therefore the attractive capillary force is

$$F = 4\pi R\sigma. \tag{3.5.3}$$

3.6 Magnetic Forces

The technique that is employed to study the magnetic properties of the sample is called the magnetic force microscopy (MFM). For high sensitivity measurements of magnetic forces, a tip made of magnetic materials such as nickel and iron is used to ensure high magnetic permeability. The magnetised tip scans the magnetic sample in non-contact mode. Information about the sample is obtained from the force of interaction between them. The magnetic energy U of the interaction between the tip and the sample is computed by integrating the dot product of the magnetisation **M** of the sample and the magnetic stray field **H** of the tip over the interaction volume V . It is given by

$$U = -\mu_0 \int_V \mathbf{M}.\mathbf{H} dV, \tag{3.6.1}$$

where μ_0 is the magnetic permeability of vacuum. The magnetisation describes the response of a material when a magnetic stray field is applied. The force can also be obtained considering the magnetisation of the tip in the presence of a magnetic stray field of the sample.

From Equation (3.6.1), the force between the tip and the sample can be computed,

$$F = \mu_0 \int_V \nabla \left(\mathbf{M}.\mathbf{H}\right) dV. \tag{3.6.2}$$

4. Kelvin Probe Force Microscopy

Kelvin probe force microscopy is a famous techniques that was first developed by Nonnenmacher et al. (1991). It is known for mapping the surface electrical properties such as the work function of a material, for-example semiconductors, on a nano-meter scale. For the commonly studied quantity is the contact potential difference (CPD). In 1898, Lord Kelvin (Sadewasser and Glatzel, 2012) studied a set of vibrating parallel plates with different Fermi energies. He connected the plates with a conducting wire, a current equalising the Fermi energies was measured. Then a voltage was applied between the plates and altered such that no current current was measured any more. The voltage corresponds to the CPD.

In 1991 Nonnenmacher, combined the atomic force microscopy with the Kelvin probe technique considering the electric force and the electric force gradient between the tip and the sample (the tip and sample is considered as a parallel plate capacitor) after its success the Kelvin probe force microscope was developed. The electrostatic force instead of current is measured because the plates at a microscopic scale are too small to give sufficient currents.

Figure 4.1 is an energy band diagram showing the different three situations a,b and c of the experiment. The set up explains the mechanism of KPFM, and how the work function can be obtained.

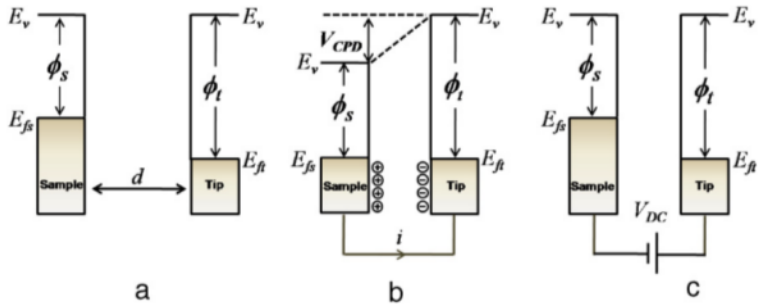

Figure 4.1: An energy band diagram for a tip and sample at different Fermi energies E_{ft}, E_{fs} and different work functions ϕ_t and ϕ_s respectively, where in case (a) the tip and sample are not connected, (b) the tip and the sample are connected with a conducting wire and (c) a voltage is applied between the tip and the sample. The diagram is taken from (Melitz et al., 2011)

In this experiment, the tip and the sample separated by a distance d as in Figure 4.1 (a) have different work functions. Work function is defined as the minimum amount of energy required by an electron to leave a metal surface. The Fermi levels are not in equilibrium. When a conducting wire is connected between the tip and the sample, electrons flow from the sample which has low work function leaving the sample positively charged to the tip with higher work function. The Fermi levels are equalised and an electric field is formed with the contact potential difference V_{CPD} as in 4.1(b). In Figure 4.1(c) a battery of voltage V_{dc} is connected between the tip and sample. The electric force between the tip and the sample goes to zero if the applied voltage is equal to the to the contact potential difference (i.e., $V_{CPD} = V_{dc}$) which is related to the work function as

$$V_{CPD} = \frac{\triangle\phi}{-e} = \frac{\phi_s - \phi_t}{e}, \tag{4.0.1}$$

where e is the electric charge of an electron.

KPFM operates in the dynamic mode of AFM where the cantilever of the AFM has a high force sensitivity which results in high sensitive surface potential measurements. The KPFM works with two different imaging modes, that is the amplitude modulation (AM) and the frequency modulation (FM) considering the electric force and the force gradient, respectively (Sadewasser and Glatzel, 2012). The KPFM can be implemented in either a dual-pass mode or a single pass-mode. In the dual-pass mode (lift mode) the first pass measures the topography while in the second pass the work function is measured with the cantilever lifted a few nm above the sample. In the single-pass mode, the topography and the surface potential of a material can be measured simultaneously on one scan line.

4.1 Electrostatic Force and Force Gradient

For the AM-KPFM and the FM-KPFM, in addition to the compensation voltage V_{dc}, an alternating voltage $V_{ac}\sin\omega t$ is applied between the tip and the sample at the cantilever's resonance frequency ω. We have seen already in Equation (3.4.3) that the electric force between the tip and sample is given by

$$F = -\frac{1}{2}\frac{\partial C}{\partial z}\triangle V^2, \tag{4.1.1}$$

$\triangle V$ is the difference between the bias voltages and the contact potential difference.

$$\triangle V = V_{dc} + V_{ac}\sin\omega t - V_{CPD}. \tag{4.1.2}$$

If we substitute Equation (4.1.2) into (4.1.3) we obtain,

$$F = -\frac{1}{2}\frac{\partial C}{\partial z}\left(V_{dc} + V_{ac}\sin\omega t - V_{CPD}\right)^2, \tag{4.1.3}$$

The total electric force F can be written as $F = F_{dc} + F_{\omega} + F_{2\omega}$ with

$$F_{dc} = -\frac{1}{2}\frac{\partial C}{\partial z}\left((V_{dc} - V_{CPD})^2 + \frac{1}{2}V_{ac}^2\right), \tag{4.1.4}$$

$$F_{\omega} = -\frac{\partial C}{\partial z}\left(V_{dc} - V_{CPD}\right)V_{ac}\sin(\omega t), \tag{4.1.5}$$

$$F_{2\omega} = \frac{1}{4}\frac{\partial C}{\partial z}V_{ac}^2\cos(2\omega t). \tag{4.1.6}$$

The force term F_{dc} is employed to measure the topography of the sample. Employing F_{ω}, the contact potential difference can be measured. The CPD is achieved if $V_{dc} = V_{CPD}$,i.e., $F_{\omega} = 0$. The last term $F_{2\omega}$ is used for capacitance microscopy (Sadewasser and Glatzel, 2012).

It can be seen from these equations that the alternating voltage at the resonance frequency causes the electric force to modulate at ω and 2ω

Whereas in AM the force is considered, the force gradient is employed in FM. This is obtained by differentiating the electric force with respect to z,

$$F' = -\frac{1}{2}\frac{\partial^2 C}{\partial z^2}\left(V_{dc} + V_{ac}\sin\omega t - V_{CPD}\right)^2. \tag{4.1.7}$$

The force gradient can be written as,

$$F' = -\frac{1}{2}\frac{\partial^2 C}{\partial z^2}\left((V_{dc} - V_{CPD})^2 + \frac{1}{2}V_{ac}^2\right) - \frac{1}{2}\frac{\partial^2 C}{\partial z^2}\left(V_{dc} - V_{CPD}\right)V_{ac}\sin(\omega t) + \frac{1}{4}\frac{\partial^2 C}{\partial z^2}V_{ac}^2\cos(2\omega t) \tag{4.1.8}$$

The middle term vanishes when $V_{dc} = V_{CPD}$. This can be used to measure the potential in the FM-KPFM.

4.2 AM-Kelvin Probe Force Microscopy

The ac-voltage is applied between the cantilever and the sample. This gives rise to the electric force between the tip and the sample. The cantilever is mechanically oscillating at its resonant frequency ω_0. The ac voltage is then chosen to be the resonant frequency of the cantilever. This causes the cantilever oscillate at ω. The oscillations are detected by the position sensitivity photodiode. The amplitude of the cantilever's oscillation at ac-frequency ω is measured, the system is more sensitive to the force F_ω and allows to lower the ac-voltage (Sadewasser and Glatzel, 2012). The frequency signal from the position sensitivity photo-detector is fed into the lock-in amplifier which detects the amplitude of the oscillation. The signal is then fed into the KPFM feedback loop as seen in Figure 4.2. The feedback adjusts the V_{dc} until the amplitude of oscillation of the force F_ω goes to zero. At this point the force term F_ω in Equation (4.1.4) is zero

$$F_\omega = -\frac{\partial C}{\partial z}\left(V_{dc} - V_{CPD}\right) V_{ac} \sin(\omega t) = 0. \tag{4.2.1}$$

Hence the output signal is used to map the information about the contact potential difference.

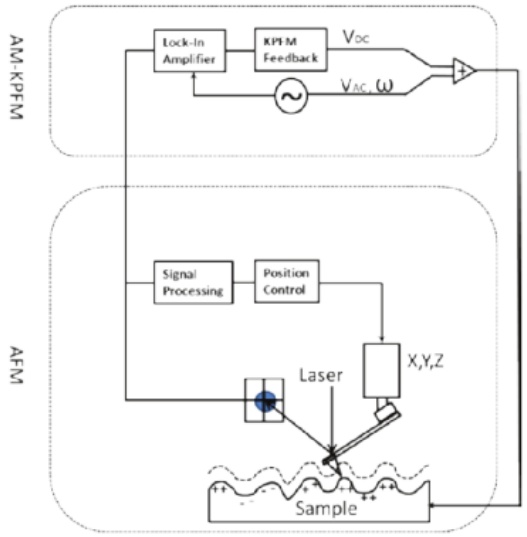

Figure 4.2: Amplitude modulation in the Kelvin Probe force microscopy, where the applied alternating voltage between the tip and the sample at the resonant frequency ω, its at this same frequency that the cantilever is oscillating. The figure is taken from(Li et al., 2013)

The technique measures the topography and the CPD in a dual-pass mode. The topography is measured from the mechanical oscillation of the cantilever at ω_0 and V_{ac} oscillates at ω to measure the CPD.

4.3 FM-Kelvin Probe Force Microscopy

In the FM-KPFM, when the electric force gradient is measured due to the applied ac-bias, the resonant frequency of the cantilever between the ac-bias frequency ω and the second harmonic 2ω is modulated

as depicted in Equation (4.1.8). Now, when the cantilever is mechanically excited at the resonance frequency ω and an ac-bias is applied simultaneously at frequency ω_m, a spectrum is obtained with the resonance frequency ω and two pairs of side-bands at $\omega \pm \omega_m$ and $\omega \pm 2\omega_m$ as in Figure 4.3.

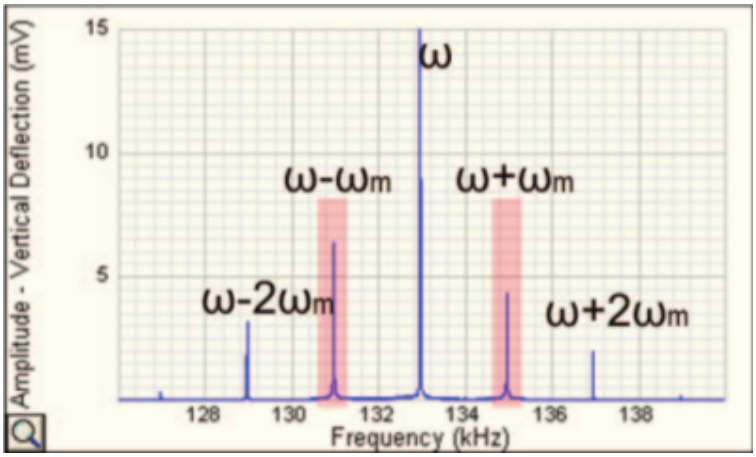

Figure 4.3: Amplitude-frequency spectrum showing two pairs of resonant peaks side by side at $\omega \pm \omega_m$ and $\omega \pm 2\omega_m$ (Li et al., 2013).

The band with frequency ω is used to measure the topography of the sample and the side band at $\omega \pm \omega_m$ is fed to the feedback loop, with the dc-voltage adjusted the CPD is obtained at $V_{cd} = V_{CPD}$

In an experimental setting, two lock-in amplifiers as seen in Figure 4.4 are used. The first amplifier locks at the resonant frequency, the output phase is then fed into the second lock-in amplifier that is tuned to the ac-bias frequency ω_m. The amplifier detects the magnitude of the frequency shift as in Equation (2.4.18), The shift is proportional to the force gradient, the formulation of the shift is given by

$$\triangle\omega = \frac{\omega}{2k}\frac{\partial^2 C}{\partial z^2}\left(V_{dc} - V_{CPD}\right)V_{ac}\sin(\omega_m t) - \frac{\omega}{2k}\frac{1}{4}\frac{\partial^2 C}{\partial z^2}V_{ac}^2\cos(2\omega t). \tag{4.3.1}$$

To decrease the crosstalk between the topography and the CPD measurement, the frequency ω_m must be large enough (Sadewasser and Glatzel, 2012).

The signal out of the second amplifier measures total amplitude of $\omega \pm \omega_m$. The output signal is what is fed into the feedback loop, to adjusts the V_{dc} until $V_{dc} = V_{CPD}$.

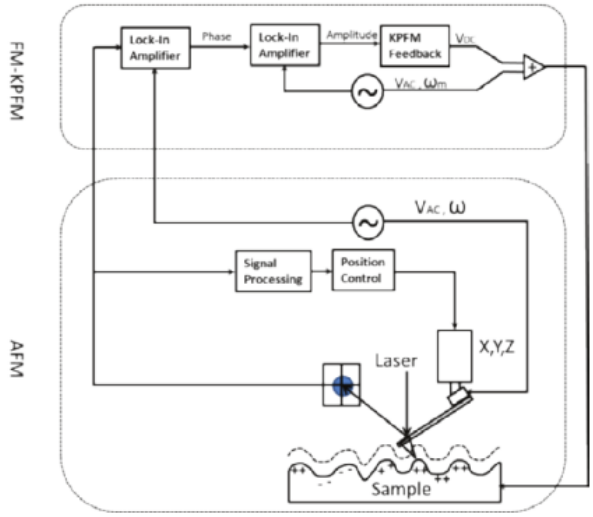

Figure 4.4: A figure for the frequency modulation in the Kelvin Probe force microscopy, where an ac-voltage is applied to the XYZ-scanner at the resonant frequency ω, an ac-bias at frequency ω_m that is responsible for modulating the resonant frequency is applied between the tip and the sample . The two lock-in amplifiers are used to total up the amplitude of side band pairs. The figure is taken from (Li et al., 2013)

4.4 Applications of KPFM

The KPFM is an imaging technique that studies the electrostatic force and surface potential of a material at a high resolution. Due to its efficiency, there a number of applications of this technique in the field of material science. With the KPFM, researchers have studied the work function of materials. The work function of a certain material helps to investigate the crystalline structure, changes in temperature of surface of a material and the material surface contaminations. These give insights into the physical and chemical properties of a material.

KPFM can also be helpful in surface photovoltaic spectroscopy. KPFM can also be helpful in studying surface states and defects under different ambient conditions. The technique can also be applied for characterising the electrical properties of semiconductor devices like solar cells, resistors, light emitting diodes (LEDs), high electron mobility transistor.

5. Bruker Multimode 8 And Its Imaging modes

In this chapter, we discuss the Bruker Multimode 8 microscope imaging modes which will be employed in future experimental studies. The Bruker Multimode 8 (BMM8) is an advanced AFM microscope that was developed by Bruker in 2010 and it has been approved for its high reliability and good performance. BMM8 provides researchers with highest resolution and fast topography imaging.

Unlike the traditional tapping mode of AFM, BMM8 operates in the PeakForce tapping mode where the cantilever oscillates at a frequency lower than the resonance frequency (nad Stefan Kaemmer and hunzeng Li f, 2011) . The microscope is equipped with a pico-force Newton scanner for force spectroscopy. This enables researchers to obtain accurate force measurements at the pico-Newton scale. Hence even the most delicate samples can be studied using BMM8.

The system is equipped with cameras for viewing the surface of the sample. This facilitates to study a particular region of interest of the sample.

5.1 PeakForce Tapping Mode (PFT)

PeakForce tapping operates similarly to the tapping mode in AFM. However, in PeakForce tapping, the lateral forces are avoided in the intermittent contact between the tip and the sample. By contrast PeakForce tapping does not operate in the resonant mode.The cantilever is rather oscillated at a frequency way below the resonant frequency, varying the z-position at small amplitudes. The interaction force is measured directly by the cantilever deflection. The measured tip-sample pico-Newton interaction force is very small. This allows for the highest resolution imaging.

During the scan, in each tapping cycle, a different force curve is measured. For every force curve PeakForce is used as a feedback signal. This gives information about the different properties of the material.

During the scan, the tip-sample force and z-position as a function of time is obtained. A visualisation of the force against time curve is shown in figure 5.1, The tip approaches the sample first and when it is withdrawn from the sample in the vertical direction.

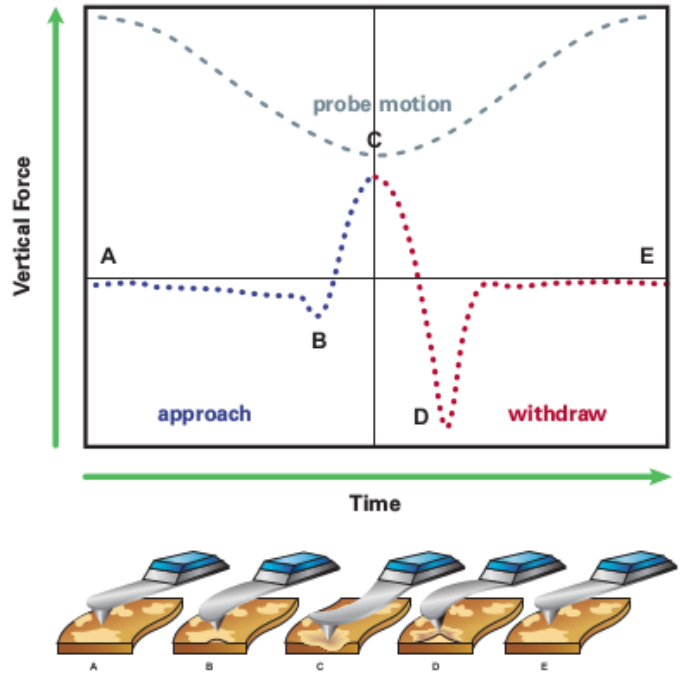

Figure 5.1: A plot of force and position against time. Point(B) corresponds to the jump-to-contact, (C) the PeakForce and (D) adhesion force (Bruker, 2012)

Figure 5.1 shows one period of the tip sample interaction. The top dashed blue curve shows the z-position of the cantilever for one period as a function of time. The lower curves (blue and red) are the force curves, showing force interactions as the tip approaches the sample and when the tip is withdrawn from the sample. The blue dashed curve indicates the approach and the red dashed curve represents the withdraw (retract).

The time for the sample to move from point A to E is given by

$$T = \frac{1}{f}, \tag{5.1.1}$$

where f is the frequency of oscillation of the cantilever.

At point A, the tip is far from the sample surface and the force of interaction is nearly zero, but as the tip approaches the sample surface, the cantilever is attracted to the surface by the attractive interaction forces. The tip is then brought into contact with the sample at B. The force starts to increase (repulsive forces) until the tip reaches the surface at point C. At point C, the cantilever is also at maximum amplitude in the z-position motion. It is at this point where we have the PeakForce which is used as a feedback signal. When the tip is withdrawn from the surface, the force (repulsive) starts to decreases until point D is reached. At this point the measured force is the adhesion force (attractive force), which can be used to map the adhesion of a material.

At point D, the tip leaves the sample surface, as indicated in Figure 5.1. From point D to point E the tip is furthest away from the sample, the forces of interactions are long range forces. At point E the force is nearly zero.

5.1.1 Force-distance curves. Graph 5.1 is recast into a force against z-position curve (see Figure 5.2) which can be used for mapping the topography of the sample. From this curve we can further extract the force against tip-sample separation (see Figure 5.3). This is then used to measure the mechanical properties like elastic modulus, adhesion, dissipation and deformation of a sample.

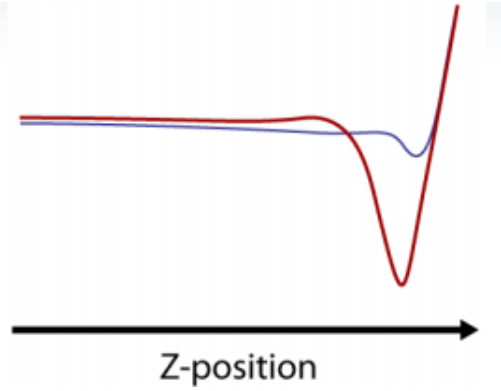

Figure 5.2: Force as a function of the z-position of the cantilever oscillations. Figure taken from (Hua, 2012).

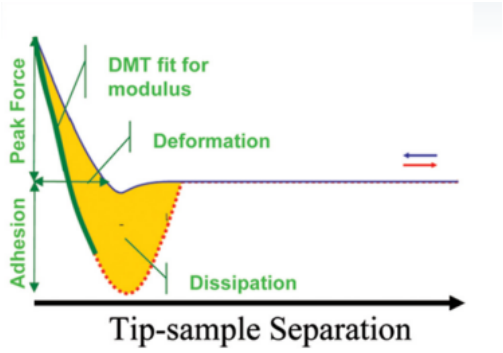

Figure 5.3: Force as a function of tip-sample seperation. Figure taken from (Hua, 2012).

Figure 5.3 allows researchers to study the mechanical properties of a sample. This can be done by fitting models like the Derjanguin-Muller-Toporov(DMT) model to the obtained curves. DMT is especially helpful for obtaining the elastic modulus (Pittenger et al., 2012). The details of this model are discussed in section 5.3.

5.1.2 Tapping mode Vs PeakForce Tapping mode. PFT is a great improvement with respect to the challenges in the tapping mode. PFT's ability to control the force of interaction, allows for the lowest forces to be detected. This helps in protecting the tip and the sample from damage. With this capability, even fragile samples can be studied.

In tapping mode, the cantilever's amplitude varies depending on the nature of interaction force (short-range or long range forces), which provides data for the topography of the sample. For PFT, the topographical data measurements is in the range B to D shown in figure 5.1. The acting forces in these regions are only short-range forces which are responsible for high-resolution imaging. This allows PFT to provide high-quality image.(Kaemmer, 2011).

In contrast to the tapping mode, PeakForce facilitates to investigate samples with complicated structures. For example, the cross-section of a sample depicted in figure 5.4. Tapping mode is not efficient for imaging such kind of samples. This is because of the geometry of the sample, which might cause the cantilever to stick on the sides of the narrow depressions on the sample, spoiling a full scan of the sample. Less information of the sample is obtained in such areas. In PeakForce tapping, even the deepest end of the depression can be probed, giving adequate information about the topography of the sample (Kaemmer, 2011).

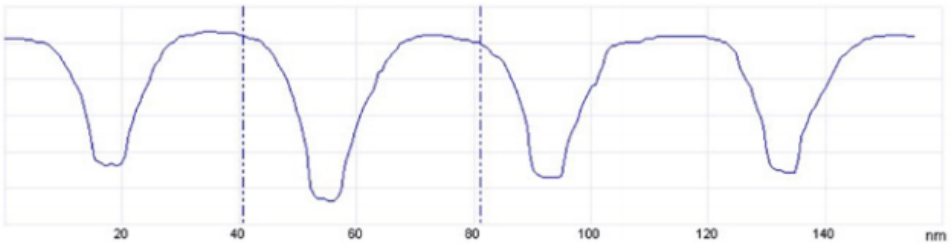

Figure 5.4: A cross-section of a sample with narrow depressions scanned in PFT. The probe even reaches even the bottom of the depressions, the sample is scanned over 160nm scan lines (Kaemmer, 2011).

Within the PeakForce Tapping mode, there are a couple of possible imaging modes which give researchers enough information to characterise different properties of a sample. PeakForce ScanAsyst is an algorithm that allows for automatic optimisation of the feed back parameters (Kaemmer, 2011).

PeakForce QNM (Quantum Nano-mechanical Imaging) which allows to study multiple sample properties like modulus, adhesion, deformation and dissipation simultaneously with the topography (Pittenger et al., 2012). With PeakForce TUNA, the conductivity of delicate samples like organic photovoltaics can be probed. Peakforce KPFM allows the surface potential of a sample to be studied. Employing these modes, imaging is done at high resolution and high speed. In the preceding sections we discuss some of these imaging modes in more detail.

5.2 PeakForce ScanAsyst

ScanAsyst is an algorithm that permits imaging with automatically optimized parameters like the set point, feedback gain, scan rate and the z-limit (see screen shoot 5.5) which are important during the scan. The algorithm sets the minimum peak force for each tip- sample interaction. ScanAsyst adjusts the feedback gain, which helps in scaling the error signals. Adjusting the scan rate controls the number of lines scanned per second. The algorithm automatically adjusts the z-limit depending on the nature of the sample surface. For smooth surfaces the z-limit is reduced to an appropriate value to allow fine imaging. This enables imaging at high-quality resolution. The technology even allows for individual control of the parameters as the user may wish, some parameters can be manually adjusted as some others are under automatic adjustments.

ScanAsyst sets all parameters on the interface except for the scan size. This can be done either by selecting the area of interest on the sample or by putting the value in the field for scan size. ScanAsyst calculations in real-time are enabled by the Field programmable gate array (FPGA) chip which is embedded in the microscope's controller (Sun et al., 2010).

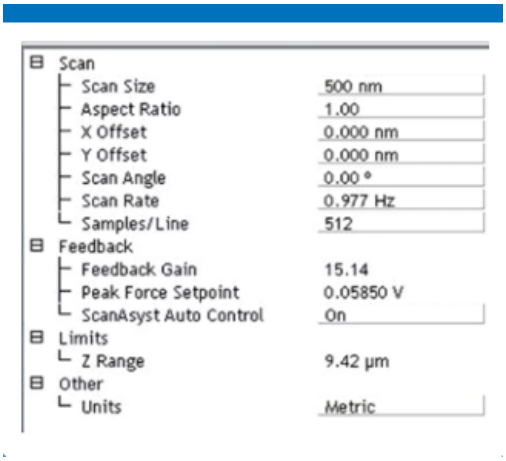

Figure 5.5: An interface for the Bruker's ScanAsyst. The parameters are under automatic adjustments except for the scan size (Bruker, 2012).

5.3 PeakForce QNM

PeakForce QNM permits to study the mechanical properties of a sample next to the topography. Within PeakFoce tapping QNM, the individual force curves of each tapping cycle are analysed with respect to different properties of a material. This is possible if the force sensor is very sensitive to allow for instantaneous measurements of the interaction force. Therefore, the cantilever must be carefully chosen such that it responds instantaneously to these forces.

In PeakForce tapping QNM, the force curves gives information about the mechanical properties (adhesion, deformation, dissipation and elastic modulus) of the sample. The collected data for each curve is fed into the data channel where imaging is done continuously. The properties of a material are mapped images. PeakForce QNM allows for imaging multiple properties at the same time.

Researchers can use the raw data to study these properties, by fitting appropriate models. The raw data is captured using the "High-speed Data capture function" (Pittenger et al., 2012). Figure 5.3 shows these properties extracted which are discussed in the following.

5.3.1 Elastic modulus. As mentioned earlier the elastic modulus is extracted by fitting a DMT model to the withdraw curve depicted in Figure 5.3. The DMT model assumes a spherical tip with radius R probing the sample. The model fits the equation

$$F - F_{adh} = \frac{4}{3} E^* \sqrt{R\delta^3} \tag{5.3.1}$$

to the force-separation curve data obtained when the tip is withdrawn from the sample. δ is the deformation of the sample, $F - F_{adh}$ is the force minus the adhesion force. E^* is the reduced Young's modulus and it is given by

$$E^* = \frac{1}{\left(\frac{1-\nu_s^2}{E_s} + \frac{1-\nu_t^2}{E_t}\right)}. \tag{5.3.2}$$

E_s and E_t are the Young's moduli of the sample and the tip respectively, ν_s and ν_t are the Poisson ratios for the sample and the tip, respectively.

If we consider a fragile sample and a stiff tip, then $E_s << E_t$. This leads to

$$E^* = \left(\frac{E_s}{1 - \nu_s^2} \right). \tag{5.3.3}$$

The model of choice is dependent on the geometry of the tip. DMT assumes a spherical tip. It may not be applicable when the tip is not spherical.

5.3.2 Deformation. The depth of tip into the sample surface at peak force corresponds to the maximum deformation. When the force on the tip increases, the deformation increases and the maximum deformation is attained at the maximum force (peak force). The deformation is recorded in each taping cycle. The measured deformation may include both elastic and plastic deformations. In Figure 5.3, deformation is indicated as the difference in tip-sample separation between the point where the force is zero on the approach curve and the point where the force is maximum.

5.3.3 Adhesion. From the curve in figure 5.3, the adhesion force corresponds to the maximum negative force. Attractive forces such as Van dar Waals forces could be a possible contribution to adhesion forces. The common contribution is the earlier discussed capillary force. The adhesion increases with the tip's radius, this can be seen in the equation (3.5.3). The adhesion channel maps the adhesion force for each tapping curve.

5.3.4 Dissipation. From the force-separation curve, the dissipation energy is the area shaded yellow in Figure 5.3 between the approach curve and the withdraw curve. The dissipation energy is the work done by the interaction force in a cycle. This energy is given by

$$\int \mathbf{F}.d\mathbf{z}, \tag{5.3.4}$$

where **F** is the force of interaction, $d\mathbf{z}$ is the displacement vector. The integral goes to zero if the approach and withdraw curve coincide. The dissipation channel plots the dissipated energy for each tapping cycle.

PeakForce QNM measures quantitative elastic modulus between 1 MPa and 20 GPa properly. For this range of values to be achieved, it is necessary that the selected cantilever is calibrated, the calibration of the cantilever ensures the quality results. The calibration can be conducted in two different ways, using the relative calibration method or the absolute calibration method.

In the relative calibration method, accumulated errors are avoided. This reduces possible errors in the measurement of the properties. For this method we need a reference sample that can be measured with the same probe as the sample to be studied. By scanning the reference sample. The reference sample is used to set the deformation depth, which should match with the PeakForce set point during imaging of the sample to be studied. The spring constant of the cantilever is measured by use of a thermal noise method as seen section 2.2.

Using the absolute method, there is no need for a reference sample, but measurements of the tip radius and the spring constant of the cantilever are required to be accurate. The spring constant is measured with thermal tune (thermal noise method) and for the tip radius see calibration of cantilever in section 2.2 . In both methods(relative calibration and absolute calibration) measurements of the deflection sensitivity of the cantilever is required see section 2.2.

5.4 PeakForce TUNA

PeakForce TUNA (PF-TUNA) is a Bruker development whose operation is based on the PeakForce tapping mode. PF-TUNA is designed to study conductivity of even fragile materials. Since the force interactions can be controlled, there are no lateral forces. This facilitates a high resolution in current imaging. In addition to the conductivity of samples, PF-TUNA can also image the nano-mechanical properties of a sample.

The set up in figure 5.6 that illustrates how PF-TUNA simultaneously maps the current of the sample and its mechanical properties. A conductive AFM probe scans the sample surface in the PeakForce

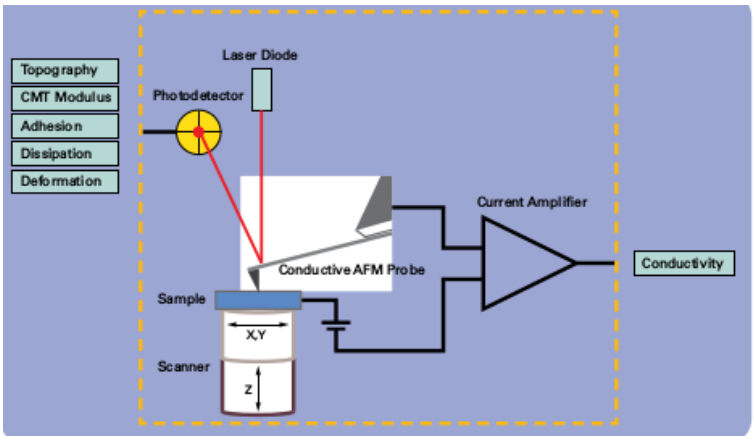

Figure 5.6: PeakForce TUNA scheme (Li et al., 2011)

tapping mode. When a dc-voltage is applied between the probe and the sample an electric field is formed. The module uses the current amplifier to detect the current

$$I = JA, \tag{5.4.1}$$

through the sample where J is the current charge density and A the area through which electrons flow. The detected current is used to measure the conductivity of the sample simultaneously with the mechanical properties of the sample.

The PeakForce algorithm collects the peak force and the current per tapping cycle. The force as a function of time curves and the current as a function of time curves are obtained for each cycle. Information from each tapping cycle collectively contributes to the properties of the samples, which allows mapping of these properties. The plot of the z-position, force and current as function of time per cycle is shown in Figure 5.7

We already discussed how the mechanical properties like elastic modulus, adhesion, dissipation and deformation can be extracted from the curves of z-position and force as a function of time in PeakForce QNM. Therefore, we only consider the current-time curve. There are three measurements that are extracted from the curves. These are the peak current, contact current and the TUNA current (Li et al., 2011).

The peak current is extracted at a point where the tip-sample interactions register maximum force (Peak force). Unlike the peak force, the peak current does not necessarily correspond to the maximum current. This is because of the small time it takes to attain the peak force, which results to a current lag. The peak current is recorded for each tapping cycle.

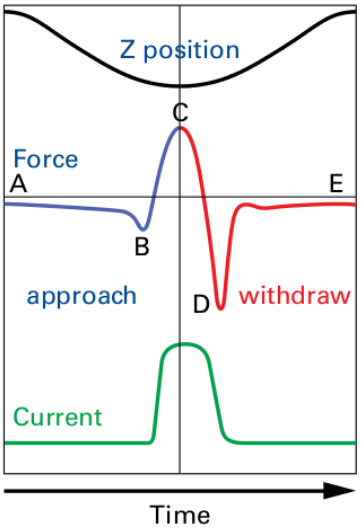

Figure 5.7: An illustration of force curve, z-position and current depending on the time for a full cycle in PF-TUNA (Li et al., 2011)

The contact current is the average current when the tip is in contact with the sample. This happens between point B (tip approaches the sample surface) and point D (where the tip sets off the sample surface). The contact current is extracted for every cycle.

The TUNA current also known as the cycle-averaged current, is extracted by averaging the current over the entire cycle from A to E. It caters for the TUNA current when the tip and sample are in contact and when the tip and sample are not in contact. The current is registered for each cycle and fed into the current channel for mapping.

Besides the imaging modes, PeakForce TUNA can also use the spectroscopy mode (Li et al., 2011). In the spectroscopy mode, the I-V spectra is used to determine the sample conductivity. In this mode, the tip is kept at a fixed position as the sample is moved up and down by the applied voltage between the tip and the sample. The feedback loop maintains a constant deflection. The current I measured from the current amplifier (see in Figure 5.6) is plotted against voltage V.

5.5 PeakForce KPFM

PeakForce KPFM is a high resolution imaging technique that combines the FM-KPFM and the PeakForce tapping mode. The combination provides scientists with more information about the sample. PeakForce KPFM tapping mode allows to study the mechanical properties employing the PeakForce QNM. In addition the topography and the surface potential can be measured. The mechanism remains the same for obtaining the mechanical properties as discussed earlier, see Figure 5.3. For the KPFM, it is more efficient to have the scan in the dual pass mode. In FM-KPFM, the phase of oscillation measures the frequency shift. In case of direct contact between the tip and the sample, a sharp phase change is registered. This leads to errors in the mapping of the surface potential. Within the PeakForce tapping mode, a light tapping is implemented. PeakForce tapping ensures reduced artifacts (errors in the mapping). The reason for recommending a dual pass is that, even with this light tapping, some phase contrast might be strong for the single pass to remove the phase cross talk (Li et al., 2013). In

the dual pass, the PeakForce KPFM can be uselful in identifying possible artifacts as the lift height of the tip is adjusted. This allows the user to lift the tip until a scan with reduced artifacts is obtained.

Conclusion s

We have presented AFM as a technique that studies materials at a nano scale. We have discussed its working principal, working modes like the contact mode, non-contact mode and the tapping mode. The interaction forces are classified as attractive and repulsive force. We have discussed the dynamics of the cantilever analytically for the amplitude of oscillation, the phase and the shift in the resonance frequency.

AFM combined with Kelvin Probe technique, maps the topography, surface potential properties, nano mechanical properties of a material. Comparisons in efficiency of the technique in studying materials depending on the mode of operation is made.

The PeakForce tapping mode, is mentioned as the most efficient one, with high image resolution and fast imaging which is suitable for more delicate samples compared to the tapping mode and the contact mode. With the PeakForce tapping mode we have presented the possibilities of extracting nano mechanical properties next to other properties such as surface potential and conductivity in PeakForce KPFM and PeakForce TUNA, respectively. Force curves have been presented as the heartbeat behind extracting these properties.

In future work, semiconductor nano wires of III-V semiconductor materials for solar cells will be experimentally studied with the technique in order to improve on the efficiency solar cells.

Acknowledgements

I take this opportunity to thank AIMS-Tanzania for giving me this opportunity to pursue my structured masters degree. I also want to thank Professor Erkki Lähderanta for the directions and comments during this study. It is my pleasure to thank Dr. Julia Borchardt for the support and encouragement rendered to me from the beginning to the end of my work. I want to thank Dr Pavel Geydt for comments to improve on my work. Finally, I extend my thanks to my family and friends for the encouragements and support.

References

J. Adamcik, C. Lara, I. Usov, J. S. Jeong, F. S. Ruggeri, G. Dietler, H. A. Lashuel, I. W. Hamley, and R. Mezzenga. Measurement of intrinsic properties of amyloid fibrils by the peak force qnm method. *Nanoscale*, 4(15):4426–4429, 2012.

G. Binnig, H. Rohrer, C. Gerber, and E. Weibel. Surface studies by scanning tunneling microscopy. *Physical review letters*, 49(1):57, 1982.

G. Binnig, C. F. Quate, and C. Gerber. Atomic force microscope. *Physical review letters*, 56(9):930, 1986.

Bruker. Absolute vs. relative calibration methods. *ww.nanophys.kth.se*, 2011.

Bruker. Peakforce tapping. *How AFM Shold Be*, 14, 2012.

H.-J. Butt, B. Cappella, and M. Kappl. Force measurements with the atomic force microscope: Technique, interpretation and applications. *Surface science reports*, 59(1):1–152, 2005.

P. Eaton and P. West. *Atomic Force Microscopy*. Number 256 in Academic: Science. Oxford University Press, 2010.

J. C. Eijkel and A. Van Den Berg. Nanofluidics: what is it and what can we expect from it? *Microfluidics and Nanofluidics*, 1(3):249–267, 2005.

R. García. *Amplitude modulation atomic force microscopy*. John Wiley & Sons, 2011.

R. Garcıa and R. Perez. Dynamic atomic force microscopy methods. *Surface science reports*, 47(6): 197–301, 2002.

Y. Hua. Peakforce-qnm advanced applications training 2014. *Technical Support Engineer*, 2012.

J. N. Israelachvili. *Intermolecular and surface forces*. Academic press, 2011.

S. B. Kaemmer. Introduction to bruker's scanasyst and peakforce tapping afm technology. *Application Note # 133*, 14, 2011.

C. Li, S. Minne, B. Pittenger, A. Mednick, and B. N. S. Division. Simultaneous electrical and mechanical property mapping at the nanoscale with peakforce tuna. *Application Note # 132*, 14, 2011.

C. Li, S. Minne, Y. Hu, J. Ma, J. He, H. Mittel, V. Kelly, N. Erina, S. Guo, and T. Mueller. Kelvin probe force microscopy. *Application Note # 140*, 14, 2013.

Y. Martin and H. K. Wickramasinghe. Magnetic imaging by "force microscopy" with 1000 å resolution. *Applied Physics Letters*, 50(20):1455–1457, 1987.

W. Melitz, J. Shen, A. C. Kummel, and S. Lee. Kelvin probe force microscopy and its application. *Surface Science Reports*, 66(1):1–27, 2011.

E. Meyer. Atomic force microscopy. *Progress in surface science*, 41(1):3–49, 1992.

N. E. nad Stefan Kaemmer and hunzeng Li f. Multimode 8. *The Benchmark for High-Performance AFM, Now with High-Speed ScanAsyst*, 14, 2011.

M. Nonnenmacher, M. o'Boyle, and H. K. Wickramasinghe. Kelvin probe force microscopy. *Applied physics letters*, 58(25):2921–2923, 1991.

R. Perez. Dynamic atomic force microscopy:basic concepts. Unpublished manuscript.

B. Pittenger, N. Erina, and C. Su. Quantitative mechanical property mapping at the nanoscale with peakforce qnm. *Application Note Veeco Instruments Inc*, 2010.

B. Pittenger, N. Erina, and C. Su. Quantitative mechanical property mapping at the nanoscale with peakforce qnm. *Application Note # 128*, 14, 2012.

D. Quenet. Mechanical properties of nanoparticles: Basics and applications. Physics D Applied Physics.

L. E. Reichl. *A modern course in statistical physics*. John Wiley & Sons, 2016.

S. Sadewasser and T. E. Glatzel, editors. *Kelvin Probe Force Microscopy*. Number 334 in Springer Series in Surface Sciences. Springer-Verlag Berlin Heidelberg, 1 edition, 2012.

Y. Seo and W. Jhe. Atomic force microscopy and spectroscopy. *Reports on Progress in Physics*, 71(1): 016101, 2007.

Y. Sun, Y. Fang, Y. Zhang, and X. Dong. Field programmable gate array (fpga) based embedded system design for afm real-time control. *2010 IEEE International Conference on Control Applications*, pages 245–250, 2010.

M. Wainwright. Bruker multimode 8. *http://www.analytical.unsw.edu.au/facilities/bmif/instruments/bruker-multimode-8*, 2016.

Q. Zhong, D. Inniss, K. Kjoller, and V. Elings. Fractured polymer/silica fiber surface studied by tapping mode atomic force microscopy. *Surface science*, 290(1-2):L688–L692, 1993.